Motor Current Signal Analysis using a Modified Bispectrum for Machine Fault Diagnosis

Fengshou Gu[1,a], Yimin Shao[2,b], Niaoqin Hu[3,c], Bruno Fazenda[1,d], Andrew Ball[1,e]

School of Computing and Engineering, University of Huddersfiled, U.K.)
(Tel : +44-1484-473548, [a]f.gu@hud.ac.uk, [d]b.fazenda@hud.ac.uk, [e]a.ball@hud.ac.uk
[2]Mechanical Transmission Laboratory, Chonqing University, P.R. China
(Tel : +86-23-65112529 [b]qgj@nudt.edu.cn)
[3]School of Mechatronics Engineering and Automation, National University of Defense Technology, Changsha, Hunan, P. R. CHINA
(Tel : +13873143967 [c] chnq@nudt.edu.cn)

Abstract: This paper presents the use of the induction motor current to identify and quantify common faults within a two-stage reciprocating compressor. The theoretical basis is studied to understand current signal characteristics when the motor undertakes a varying load under faulty conditions. Although conventional bispectrum representation of current signal allows the inclusion of phase information and the elimination of Gaussian noise, it produces unstable results due to random phase variation of the sideband components in the current signal. A modified bispectrum based on the amplitude modulation feature of the current signal is thus proposed to combine both lower sidebands and higher sidebands simultaneously and hence describe the current signal more accurately. Based on this new bispectrum a more effective diagnostic feature namely normalised bispectral peak is developed for fault classification. In association with the kurtosis of the raw current signal, the bispectrum feature gives rise to reliable fault classification results. In particular, the low feature values can differentiate the belt looseness from other fault cases and discharge valve leakage and intercooler leakage can be separated easily using two linear classifiers. This work provides a novel approach to the analysis of stator current for the diagnosis of motor drive faults from downstream driving equipment.

Keywords: Modified Bispectrum, Kurtosis, Induction Motor, Current Signature Analysis, Reciprocating Compressor

1. INTRODUCTION

Induction machine stator current signals have been used widely to determine the health of the induction machine since the early 1980's [1]. A limited amount of work has been undertaken in using the current signals to investigate the potential of using the induction machine as a means of assessing the condition of downstream driven equipment. Publications in [2-7] show many interesting achievement in this direction. In all these publications the use of the motor supply parameters for the detection of equipment train faults has been limited in that no deterministic approaches have been demonstrated. One of the main reasons for this lack of diagnostic clarity is that the harmonic content and noise contained within an induction machine supply parameter, and in particular the stator current, is high and that traditional two-dimensional spectral analysis techniques can be insufficient to properly correlate the stator current data with faulted conditions.

Higher Order Spectra (HOS) are useful signal processing tools that have shown [8-9] significant benefits over traditional spectral analyses because of non-linear system identification, phase information retention and Gaussian noise elimination properties. The application of HOS techniques in condition monitoring has been reported in [10-11] and it is clear that multi-dimensional HOS measures can contain more useful information than traditional two-dimensional spectral measures for diagnostic purposes. Further, in [11], it was shown that these measures could be used in a deterministic manner to predict the HOS components of induction machine vibration sensitive to a number of fault conditions. Additionally, it was demonstrated that the HOS measures were more sensitive to the fault conditions than traditional spectral analysis. However, these techniques have not been extended to include induction machine supply parameter investigations or faults on the downstream driven equipment train.

This paper begins to address these issues by investigating the capability of the induction motor phase current to detect different faults in a reciprocating compressor. Theoretical principles are presented that predict the frequency components of the motor phase current sensitive to the seeded faults. The properties of a modified bispectrum are reviewed to highlight the effectiveness in processing AM like current signals. An experimental investigation is presented and four compressor conditions are investigated over a wide range of discharge pressure conditions.

2. MOTOR CURRENT SIGNAL

Based on the analysis in [13, 14], motor current signals can be derived. To simplify analysis process, the electromagnetic relationships are examined in phase *A*, one of the three phases of power supply, and the higher harmonics in the phase is not considered. Referring to supply voltage, the current signal in phase *A* for a health motor drive can be expressed as

$$i_A = \sqrt{2} I \cos(2\pi f_s t - \alpha_I) \quad (1)$$

Correspondingly, the magnetic flux in motor stator is

$$\phi_A = \sqrt{2} \phi \cos(2\pi f_s t - \alpha_\phi) \quad (2)$$

The electrical torque produced by the interaction between the current and flux can be expressed as

$$T = 3P\phi I \sin(\alpha_I - \alpha_\phi) \quad (3)$$

where I and ϕ denote the root mean squared (RMS) amplitudes of the supply current and linkage flux respectively, α_I and α_ϕ are the phases of the current and flux referring to supply voltage, f_s is the fundamental frequency of electrical supply and P is the number of pole pairs. If there is a fault occurring in the rotor system including motor rotor and rotational components connected to the rotor mechanically, there will be an additional torque component oscillating around the electric torque. Supposing the additional torque ΔT is a sinusoidal wave with a frequency f_F and referring to Eqn. (3) and assuming the phase α_F, the oscillatory torque:

$$\Delta T = 3P\phi I_F \sin[2\pi f_F t - (\alpha_I - \alpha_\phi) - \alpha_F] \quad (4)$$

Correspondingly, this oscillatory torque causes speed fluctuation. From the motor torque balance equation, the speed fluctuation due to this oscillatory torque can be derived as

$$\Delta\omega = \frac{P}{J}\int \Delta T dt = \frac{3P^2\phi I_F}{2\pi f_F J}\cos[2\pi f_F t - (\alpha_I - \alpha_\phi) - \alpha_F] \quad (5)$$

and the angular oscillation is

$$\Delta\alpha_F = \int \Delta\omega dt = -\frac{3P^2\phi I_F}{4\pi^2 f_F^2 J}\sin[2\pi f_F t - (\alpha_I - \alpha_\phi) - \alpha_F] \quad (6)$$

where J is the inertia of the rotor system. This angular variation produces phase modulation to the linkage flux and Eqn. (2) becomes

$$\begin{aligned}\phi^F{}_A &= \sqrt{2}\phi\cos\{2\pi f_s t - \alpha_\phi \\ &- \Delta\phi\sin[2\pi f_F t - (\alpha_I - \alpha_\phi) - \alpha_F]\}\end{aligned} \quad (7)$$

where $\Delta\phi = \frac{3P^2\phi I_F}{4\pi^2 f_F^2 J}$. This shows that the flux wave contains nonlinear effects because of the fault in the rotor system. This nonlinear flux will produce corresponding electromagnetic force (EMF) and hence induce a nonlinear current signal in the stator.

Considering that $\Delta\alpha_F$ is very small, resulting in $\cos(\Delta\alpha_F) \approx 1$ and $\sin(\Delta\alpha_F) \approx \Delta\alpha_F$, the linkage flux now can be simplified and examined in three components explicitly:

$$\begin{aligned}\phi^F{}_A &\approx \sqrt{2}\phi\cos(2\pi f_s t - \alpha_\phi) + \sqrt{2}\phi\Delta\alpha_F\sin(2\pi f_s t - \alpha_\phi) \\ &= \sqrt{2}\phi\cos(2\pi f_s t - \alpha_\phi) \\ &+ \sqrt{2}\phi\Delta\phi\ \cos[2\pi(f_s - f_F)t - \alpha_I - \alpha_F] \\ &- \sqrt{2}\phi\Delta\phi\ \cos[2\pi(f_s + f_F)t - 2\alpha_\phi + \alpha_I - \alpha_F]\end{aligned} \quad (8)$$

Eqn. (8) shows that the flux contains not only the fundamental part but also two sidebands around the fundamental frequency. This simplified flux allows the current expression to be obtained based on motor equivalent circuit [13]:

$$\begin{aligned}i^F{}_A &= \sqrt{2}I\cos(2\pi f_s t - \alpha_\phi) \\ &+ \sqrt{2}I_l\cos[2\pi(f_s - f_F)t - \alpha_I - \alpha_F - \varphi] \\ &- \sqrt{2}I_r\cos[2\pi(f_s + f_F)t - 2\alpha_\phi + \alpha_I - \alpha_F - \varphi]\end{aligned} \quad (9)$$

where φ is the angular displacement of motor equivalent circuit impedance at supply frequency, I_l and I_r are the RMS values of the lower sideband and the upper sideband components respectively, which result from the interaction between the modulus of flux and the equivalent circuit impedance. By checking the amplitude of the sideband through spectrum calculation, various faults such as rotor bar broken and eccentricity can be diagnosed with high degree of accuracy. However, conventional spectrum just uses amplitude information and overlooks the phase effect which also contains fault information, as shown in Eqn. (9). The consequence of ignoring phase information may degrade diagnosis performance for the case of incipient faults when the sideband amplitude is very small and masked by various noise sources. This is particularly true to diagnose faults from downstream mechanical systems. However, bispectrum analysis allows the retention of amplitude and phase information, the good performance of noise suppression and the identification of nonlinear effects. This study then focuses on using bispectrum to analyse the current signals from a reciprocating compressor for the diagnosis of several common faults.

A reciprocating compressor system consists typically of an induction motor, a belt transmitter and a multi-cylinder compressor. The compressor has two basic processes during its working cycle: compression and expansion. Previous study [11] shows that the working process gives rise to a periodically varying load to the driving motor. This is due to the compressor requiring more power in compression than in the expansion. This varying load results in high oscillation in the measured current signal. According to Eqn. (9), the current signal measured can be expressed by denoting the various are the angular displacements with α_l and α_r the lower and higher sideband components respectively:

$$\begin{aligned}i^F{}_A &= \sqrt{2}I\cos(2\pi f_s t) \\ &+ \sqrt{2}I_l\cos[2\pi(f_s - f_F)t - \alpha_l] \\ &- \sqrt{2}I_r\cos[2\pi(f_s + f_F)t - \alpha_r]\end{aligned} \quad (10)$$

In Eqn. (10) two components: $f_s - f_F$ and $f_s + f_F$ are distributed symmetrically around the supply frequency, showing that the phase current signal from the compressor is similar to the form of an amplitude modulation (AM). However, because $\alpha_l \neq \alpha_r$ and $I_l \neq I_r$, Eqn.(1) is not a pure AM process. As discussed in [13, 14] The angular displacements of the sideband are linked but have an angular difference, which is governed by both the phase of magnetic linkage flux and the phase of the equivalent circuit impedance. For the similar reason their amplitudes also have some

differences. However, when angular displacements: α_l and α_r are considered individually, they will change randomly because they are influenced by the time range considered, the position of the fault on the rotor, the starting rotor position, and the rotor position evolution during the transient state to reach the speed mean value. Therefore conventional bispectrum cannot represent this type of signal adequately, as shown in section 3.

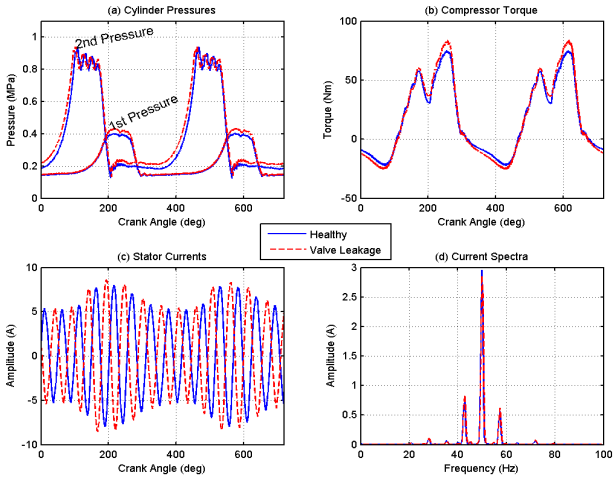

Fig. 1 Stator current waveforms and spectra for a healthy compressor and a valve leakage case

Nevertheless, the amplitude and pattern of the two sidebands will change with the degree of load fluctuation. When a reciprocating compressor runs under normal conditions the load oscillation increases with the increase of discharge pressure. This also means that if there is a fault in the compressor, the load oscillation characteristics will be altered and hence the sidebands will be different from that when compressor is healthy. Fig. 1 shows the current signals from a two-stage reciprocating compressor. The compressor has a 2.3kw three-phase four-pole induction motor, a V-belt with a transmission ratio of 3.2 and a two-stage compressor operating in a pressure range from 80psi to 120psi (5.5bar to 8.3bar). From the in-cylinder pressure waveforms and compressor torques, shown in Fig. 1(a) and (b), respectively, the motor is under a dynamic load fluctuating at about 7.3Hz according to the working cycle of the compressor. This fluctuating load leads to a amplitude modulation current waveform, shown in Fig. 1(c). The spectra of current signals, shown in Fig. 1(d), exhibit a high degree of AM feature. The carrier components at the supply frequency 50Hz has very high amplitude and the sideband components at 50±7.3Hz which correspond to the working frequency of the compressor are clearly visible.

More interestingly, the amplitude of the current waveform from the valve leakage seems slightly higher than that of healthy condition. In the spectra, the sideband amplitudes for the leakage are also slightly higher whereas the supply amplitude has a small decrease when compared with the spectrum of the healthy condition. These are consistent with the changes in the pressure and torque graphs, which mean that the current signals contain sufficient information for compressor fault detection and diagnosis.

However, the changes in current signals due to this operating condition often mask the small changes due to incipient faults. This makes it difficult to classify and quantify different types of faults. Therefore, more advanced signal processing methods have to be used to enhance the small changes by including diagnostic information in the signal as much as possible.

3. BISPECTRUM ANALYSIS

3.1 Conversional Bispectrum

Given a discrete time current signal *x(n)*, its discrete Fourier transform (DFT), *X(f)* is defined to be

$$X(f)=\sum_{n=-\infty}^{\infty}x(n)e^{-j2\pi fn} \tag{11}$$

As it is a complex number, $X(f)$ can be rewritten in the format of magnitude $|X(f)|$ and ϕ_f :

$$X(f)=|X(f)|e^{j\phi_f} \tag{12}$$

From DFT, the conventional bispectrum $B(f_1, f_2)$ can be defined in the frequency domain as[15,16]

$$B(f_1,f_2)=E\left\langle X(f_1)X(f_2)X^*(f_1+f_2)\right\rangle \tag{13}$$

where $X^*(f)$ is the complex conjugate of *X(f)* and $E\langle\ \rangle$ is the statistical expectation operator. f_1, f_2 and f_1+f_2 are three individual frequency components. Note that, unlike second-order measures, this third-order measure is a complex quantity in that it contains both magnitude and phase information about the original time signal *x(n)*. If the frequency components at f_1, f_2 and f_1+f_2 are independent components, each frequency will be characterized by statistically independent random phases distributed over $(-\pi, \pi)$. Upon statistical averaging denoted by the expectation operator $E\langle\ \rangle$ in Eqn. (13) the bispectrum will tend towards zero due to the random phase mixing effect. In this way random noise can be suppressed considerably.

On the other hand, if the three spectral components: f_1, f_2 and f_1+f_2 are non-linearly coupled to each other, the total phase of the three components will not be random at all, even though each of the individual phases are random, in particular the phases have the following relationship:

$$\phi(f_2)+\phi(f_1)=\phi(f_2+f_1) \tag{14}$$

Consequently, the statistical averaging will not lead to a zero value in the bispectrum. This nonlinear coupling is indicated by a peak in the bispectrum at the *bifrequency* $B(f_1,f_2)$.

To measure the degree of coupling between coupled components, a normalized form of the bispectrum or

bicoherence is usually used and defined as [16]

$$b^2(f_1,f_2)=\frac{\left|B(f_1,f_2)\right|^2}{E\left\langle\left|X(f_1)X(f_2)\right|^2\right\rangle E\left\langle\left|X(f_1+f_2)\right|^2\right\rangle} \quad (15)$$

The bicoherence is independent of the amplitude of the triple product of the DFT amplitudes and its values are bounded between 0 and 1. The bicoherence is close to 1 if there are nonlinear interactions among frequency combinations, f_1, f_2 and f_1+f_2. On the other hand, a value near 0 implies absence of interactions between the components. The possible amplitudes in the latter case may suggest that the components are produced independently from a system. Therefore, based on the amplitude of bicoherence the quadratic nonlinear interactions can be detected and the interaction degrees can be also measured between the coupling components.

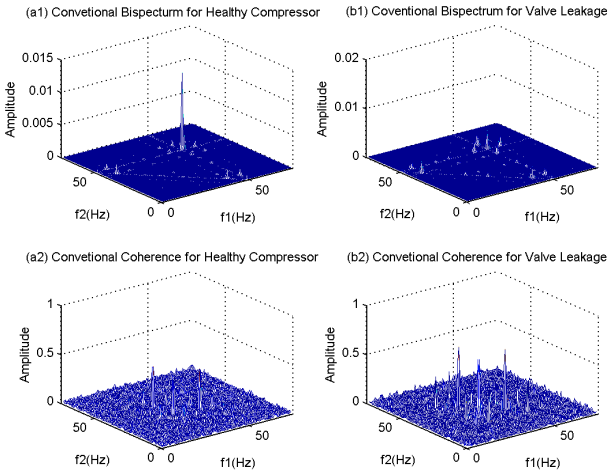

Fig. 2 Conventional bispectra for a healthy compressor and a valve leakage at 120psi(8bar)

Fig. 2 shows two bispectra and corresponding bicoherence of current signals for a healthy compressor and a valve leakage case respectively. They are calculated through a direct method using Fast Fourier Transform (FFT). The spectral resolution is 0.5Hz and the amplitude is averaged over 100 times. The two bispectra for both the healthy case and the valve leakage are very different. However, they all have a high peak at bifrequency (50, 50) and a number of small peaks which are separated by a frequency interval of 7.3Hz, arisen from the compressor working cycle and supply frequency. These feature thus may indicate the nonlinear coupling effects existing in the current signals and make difference between the normal and fault case.

According to Eqn. (13), the major component at (50, 50) results from the coupling between 50Hz, 50Hz and 100Hz. However, in theory the 100Hz component should not exist in the signal if the compressor and driving motor are fault free and hence the component is not from nonlinear coupling. This can be confirmed by the coherences shown in Fig. 2 (a2) and (b2). Their coherence amplitude for both compressor cases are close to zero values, which mean that there is not nonlinear effect at bifrequency (50, 50) component. This also indicates that the presence of 100Hz is due to background noise and spectral leakage from the finite length of DFT. Therefore, the bispectral peak at (50, 50) component is a false nonlinear coupling effect.

For similar reason, the other bifrequency components with small peaks such as those at (50-7.3, 50) and (50, 50-7.3) cannot be taken as the non-linearly effects rigorously because their corresponding coherence amplitudes are very low. As discussed in section 2, the phases of the sidebands and supply frequency vary with many influential factors and hence change between data frames for FFT calculation. The expectation average over different FFT frames will lead to a very small bispectrum magnitude at these bifrequencies. This shows that conventional bispectrum is not suitable for analysis of the current signals from the compressor.

3.2 Modified Bispectrum

Eqn. (13) includes only the presence of nonlinearity from the harmonically related frequency components: f_1, f_2 and f_1+f_2. It overlooks the possibility that the occurrence of f_1-f_2 may be also so due to the nonlinearity between f_1 and f_2. Because of this, it is not so adequate to describe AM like signals such as motor current signals. Several approaches such as [17, 18] have been developed to use bispectrum for AM signals. The modified bispectrum in [17] produces more compact results. To improve the performance of the conventional bispectrum in describing the motor current signals, this study uses the modified bispectrum [17] and names it as modulation signal bispectrum (MSB):

$$\begin{aligned}&B_{MS}(f_1,f_2)\\&=E\left\langle X(f_2+f_1)X(f_2-f_1)X^*(f_2)X^*(f_2)\right\rangle\end{aligned} \quad (16)$$

In the format of magnitude and phase, Eqn. (16) is rewritten as

$$\begin{aligned}&B_{MS}(f_1,f_2)\\&=E\left\langle\left|X(f_2+f_1)\right\|X(f_2-f_1)\left\|X^*(f_2)\right\|X^*(f_2)\right|e^{j\phi_{MS}}\rangle\end{aligned} \quad (17)$$

The total phase of MSB

$$\begin{aligned}&\phi_{MS}(f_1,f_2)\\&=\phi(f_2+f_1)+\phi(f_2-f_1)-\phi(f_2)-\phi(f_2)\end{aligned}. \quad (18)$$

As shown in Eqn. (14), if two components f_1 and f_2 are in coupling, their phases are related as

$$\begin{aligned}\phi(f_2+f_1)&=\phi(f_2)+\phi(f_1)\\\phi(f_2-f_1)&=\phi(f_2)-\phi(f_1)\end{aligned} \quad (19)$$

By substituting (19) into (18) the total phase of MSB will be zero and MSB amplitude will be the product of the four magnitudes, which is the maximum of the complex product. Therefore, a bispectral peak will appear at (f_1, f_2). Especially, Eqn. (16) now takes into account both (f_1+f_2) and (f_1-f_2) simultaneously for measuring the nonlinearity in AM signals. If (f_1+f_2) and

$(f_1\text{-}f_2)$ are both due to nonlinearity effect between f_1 and f_2, a bispectral peak will appear at bifrequency $B_{MS}(f_1, f_2)$. This is more accurate and efficient in representing the sideband characteristics of modulation signals. In addition, the four component products may enhance signal content more and produces more robust result to random noise.

Similar to the conventional bicoherence, a normalised form of MSB or modulation signal bicoherence is

$$b^2{}_{MS}(f_1, f_2) = \frac{|B_{MS}(f_1, f_2)|^2}{E\left\langle |X(f_2)X(f_2)X^*(f_2)X^*(f_2)|^2\right\rangle E\left\langle |X(f_2+f_1)X(f_2-f_1)|^2\right\rangle} \quad (20)$$

to measure the degree of coupling between three components.

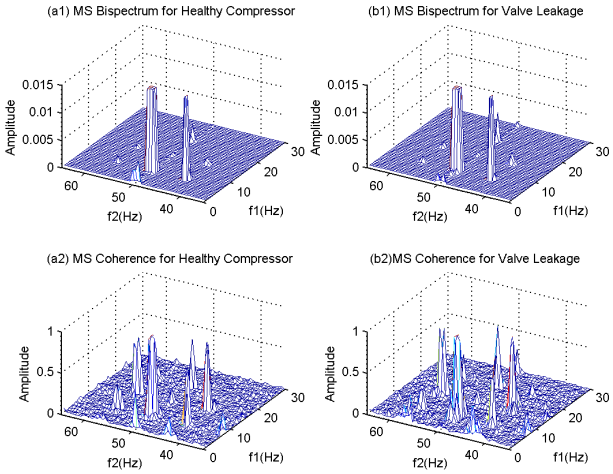

Fig. 3 MS bispectra for a healthy compressor and a valve leakage case at discharge pressure of 120 psi(8bar)

Fig. 3 shows the MS bispectra and corresponding coherences for the two current signals shown in previous section. To show small bispectral peaks, peaks higher than 0.015 are truncated to 0.015. Even though the large peak at bifrequency (7.3, 50) can be found to be higher than that at bifrequency (7.3, 50-7.3) based on the degree of peak wideness. In association with the coherence peak distribution, more peaks can be observed in the bispectral slice $f_2 = 50$Hz. These peaks show the nonlinear interaction between the supply frequency and the higher order harmonics of compressor working frequency. In particular, the peak value at (3×7.3, 50) for the faulty case is higher than that for the healthy case. This higher nonlinear effect at the harmonics can be an effective feature for fault diagnosis because different types of faults will change the load oscillation patterns in different ways and hence the peak patterns will be different.

4. FAULT DIAGNOSIS

From MS bispectrum analysis, a bispectral peak feature is developed as the average peak values around the major peak normalised by signal RMS. Fig. 4 presents the results of compressor fault separation by combining the bispectrum peak features with signal kurtosis. The top graph shows the effects of the three common faults: valve leakage, inter-cooler leakage and belt looseness, on the cylinder pressures. The valve leakage causes a slight increase in the pressures of both the first stage and the second stage cylinders whereas the inter-cooler creates a small decrease in the pressures. However, the belt looseness does not cause any changes to the cylinders pressures. This means that any cylinder pressures based detection methods such as pressure, vibration and temperature will fail in detecting this type of fault. In addition, these three seeded faults are very small. The compressor can produce the required pressure level without noticeable changes in its service performance.

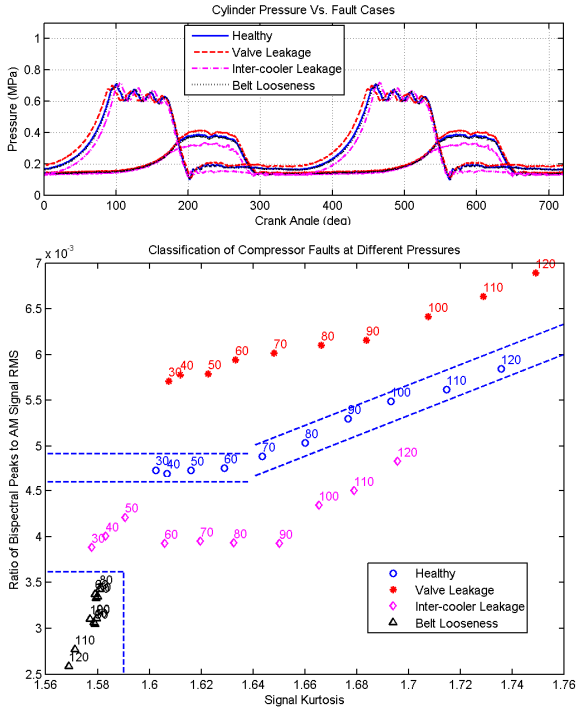

Fig. 4 Compressor fault classification under different discharge pressure

However, the suggested diagnostic features: the bispectral peak and the signal kurtosis, shown in the bottom plots of Fig. 4, show clear differences between different fault cases and the healthy operation. In addition, the differences exist over a wide discharge pressure range from 30psi to 120psi (2bar to 8bar) which covers the rated range (from 5.5bar to 8bar) of the compressor. The valve leakage produces higher values of both the bispectral peak and the signal kurtosis whereas the inter-cooler leakage shows lower values for both the features. This is consistent with the changes in cylinder pressures and the load torques. From this it can be concluded that either too high or too low feature values will indicate that a faulty or abnormal operation. In particular, the belt looseness, like the low discharge pressure operations, has very low feature values, which

shows the abnormal compressor operation.

Based on above discussions, compressor fault diagnosis can be carried out at its rated operation range from 70psi to 120psi by a linear classifier shown by the dashed line with positive slope in Fig. 4 whereas in low pressure range (30psi to 70psi) by using a static threshold to check the value of bispectral peak feature. Very low feature values can be used to differentiate the belt looseness from other fault cases. Valve leakage and inter-cooler leakage can be separated easily using two constant thresholds as shown by the dashed horizontal lines in Fig. 4.

5. CONCLUSION

The analysis of the induction motor current signal with bispectrum clearly has significant potential as a means of non-intrusively detecting the presence of incipient faults in its driven equipment items by extracting the nonlinear interaction of linkage flux due to load variation. However, the conventional bispectrum is not so adequate in representing the current signals with AM features because it cannot include sideband pairs simultaneously and the random variation of sidebands phases. A modified bispectrum i.e. MS bispectrum is then introduced to obtain a more accurate and efficient representation of the current signals. Based on the analysis, a normalised bispectral peak in conjunction with signal kurtosis is developed to diagnose common compressor faults including valve leakage, inter-cooler leakage and belt looseness. The classification results shows that the low feature values can be used to differentiate the belt looseness from other fault cases and valve leakage and inter-cooler leakage can be separated easily using two linear classifiers.

ACKNOWLEGEMENT

The authors are grateful for the financial support provided by the National Natural Science Foundation of China under Contact No.50675232.

REFERENCES

[1] W. T. Thomson, M. Fenger, “Current signature snalysis to setect induction motor faults”, IEEE Ind. Appl. Mag., Jul./Aug. 2001, pp26-34.

[2] M. E. H. Benbouzid, “A review of induction motors signature analysis as a medium for faults detection”, IEEE Trans. Ind. Elec., Vol. 47, No. 5, Oct. 2000, pp 984-993.

[3] R. R. Obaid, T. G. habetler, R. M. Tallam, “Detecting load unbalance and shaft misalignment using stator current in inverter-driven induction motors”, IEEE int. Elec. Mach. And Drives Conf., pp1454-1458, 2003.

[4] G. T. Honce, J. R. Thalimer, “Reducing unshceduled plant maintenance delays – field test of a new method to predict electric motor failure”, IEEE Trans. Ind. Appl., Vol. 32, No. 3, May/Jun. 1996, pp689-694.

[5] R.C. Kryter, H.D. Haynes, “Condition monitoring of machinery using motor current signature analysis”, Sound & Vib., Sep. 1989.

[6] K. N. Castleberry, S. F. Smith, “A dedicated compressor monitoring system employing current signature analysis”, ORNL report DE 93010270.

[7] C. Kar and A.R. Mohanty, “Monitoring gear vibrations through motor current signature analysis and wavelet transform”, Mechanical Systems and Signal Processing, Volume 20, Issue 1, pp 158-187, 2006.

[8] H. Fanglin, G. Songnian, “Application of higher order cumulant to structure fault diagnosis”, Proc. 11th Inter. Mod. Anal. Conf., pp1237-1240, 1993.

[9] G. Gelle, M. Colas, G. Delaunay, “Higher order statistics for detection and classification of faulty fan belts using acoutical analysis”, IEEE Sig. Proc. Workshop on HOS, 21-23 Jul., 1997.

[10] I. M. Howard, “Higher-order spectral techniques for machine vibration condition monitoring”, Proc. Instn. Mech. Engrs., Vol. 211, Part G, pp211-219, 1997.

[11] N. Arthur, J. Penman, “Induction machine condition monitoring with higher order spectra”, IEEE Trans. Ind. Elec., Vol. 47, No. 5, pp 1031 – 1041, Oct. 2000.

[12] M. Elhaj, F. Gu, A.D. Ball, A. Albarbar, M. Al-Qattan, A. Naid, “Numerical simulation and experimental etudy of a two stage reciprocating compressor for condition monitoring”, Mechanical Systems and Signal Processing, Vol.22 pp.374-389, Aug. 2007.

[13] F. Filippetti, G. Franceschini and C. Tassoni,, “AI techniques in induction machines diagnosis including the speed ripple effect”, IEEE Transactions on Industry Applications, Vol. 34, No. 1, pp 98-108, 1998.

[14] A. Bellini, F. Filippetti, G. Franceschini, C. Tassoni, and G.B. Kliman, “Quantitative evaluation of induction motor broken bars by means of electrical signature analysis”, IEEE Transactions on Industry Applications, Vol. 37, No. 5, pp 1248-1255, 2001.

[15] Y. C. Kim and E. J. Powers, “Digital bispectral analysis and its applications to nonlinear wave interactions,” IEEE Transactions on Plasma Science, vol. PS-7, no. 2, pp. 120–131, 1979.

[16] W. B. Collis, P. R. White, J.K. Hammond, “Higher-Order Spectra: The Bispectrum and Trispectrum”, *Mechanical Systems and Signal Processing,* Vol. 12, No.3, pp. 375-394, 1998.

[17] J.R. Stack, R.G. Hartley and T.G. Habetler, “An amplitude modulation detector for fault diagnosis in rolling element beatings”, IEEE Transactions on Industrail Electonics, Vol. 51, No. 5, pp. 1097-1102, 2004.

[18] I. Jouny and R. L. Morese, “Bispectra of modulated stationary signals”, IEE. Electronics Letters, Vol.30, No. 18, 1994, pp. 1465-1466.